Journal of Catalysis **190,** 352–363 (2000)
doi:10.1006/jcat.1999.2750, available online at http://www.idealibrary.com on IDEAL®

Influence of the Preparation Method, Outgassing Treatment, and Adsorption of NO and/or O_2 on the Cu^{2+} Species in Cu-ZSM-5: An EPR Study

J. Soria,* A. Martínez-Arias,* A. Martínez-Chaparro,* J. C. Conesa,*,[1] and Z. Schay†

*Instituto de Catálisis y Petroleoquímica, CSIC, Campus Universitario de Cantoblanco, 28049 Madrid, Spain; and †Institute of Isotopes, Hungarian Academy of Sciences, Budapest, Hungary

Received July 30, 1999; revised November 1, 1999; accepted November 2, 1999

Two Cu^{2+}-loaded ZSM-5 zeolites prepared by ion exchange from liquid solution (LS) and solid-state reaction (SR) are studied by EPR after vacuum treatments at several temperatures, T_v, up to 413 K and subsequent NO and/or O_2 adsorption. In addition to the changes in Cu^{2+} coordination upon dehydration, from octahedral to square pyramidal and planar, outgassing produced in sample LS a decrease of the Cu^{2+} EPR signal, initiated by brief outgassing at 298 K and reaching a maximum (ca. 75% of the total copper not detected) for $T_v = 383$ K. This is ascribed to fast spin relaxation, due either to a ligand geometry effect or to the establishment of copper–copper interactions. Subsequent NO adsorption at 298 K generated $(Cu–NO)^+$ complexes, apparently by reaction of square planar Cu^{2+} (possibly assisted by water or OH^- still present), while NO and O_2 coadsorption led to a large change, all copper now being EPR-visible either as a sharp signal for a square planar species or as a broad band due to spin-interacting Cu^{2+}. For sample SR, the resolved Cu^{2+} EPR signals, representing ca. 25% of the total copper, behave similarly to those found in sample LS (except that their overall intensity decreases little upon outgassing), but most copper exists as Cu-oxide clusters giving a broad EPR signal. The latter, resulting from the solid-state preparation method, seem scarcely reactive on adsorption of NO or NO + O_2; they may be connected with the lower catalytic activity in NO decomposition previously observed for this latter sample.

Key Words: **EPR; copper; ZSM-5 zeolite; dehydration; nitric oxide; solid-state exchange; coordination; clustering.**

INTRODUCTION

Cation substitution in zeolites is frequently used to modify their properties to obtain improved catalysts, ion exchange from solution being the conventional way to introduce those cations (1, 2). However, some transition metal cations are strongly solvated and their hydration shells prevent them from penetrating into the narrow channels or cavities of the zeolite structure. Considering the thermal stability of high-silica zeolite frameworks, methods based on solid-state reaction of the zeolite with some compounds of the transition metal ions of interest can overcome these difficulties (3). However, the ion-exchanged zeolites prepared by different methods and using different salts of the same transition metal cation might present different properties, because the diverse experimental conditions during the preparation can affect characteristics of the exchanged ions such as cation dispersion or ligand type. Recent studies on the catalytic properties of Cu-ZSM-5 samples prepared by ion exchange from liquid solution (LS) and by solid-state reaction (SR) have shown different activity in NO decomposition (4). With the objective of determining differences in these zeolites that could explain their different catalytic behaviour, we have studied the effect of the outgassing treatments at different temperatures on the parameters of the observed Cu^{2+} signals in detail by EPR. The study concentrates on the situation in which some water may be still present in the material (by using low or moderate outgassing temperatures), since most practical processes of NO elimination refer to combustion processes which liberate important amounts of water vapor, which is known to influence significantly the catalytic activity of Cu-loaded zeolites for NO conversion. Modifications of the EPR parameters usually indicate changes in the Cu^{2+} coordination, as has been reported by authors who have studied this type of zeolite by EPR (5–9). Understanding the evolution of the Cu^{2+} coordination with the outgassing treatments and the changes induced by subsequent adsorption steps will help to determine the differences in the copper species formed in the zeolite as result of two different cation-exchange methods. On the other hand, if (some of) the Cu^{2+} species present in the two zeolites are different, their detailed study, in connection with the results of NO or NO plus O_2 adsorption experiments, might explain the previously observed different reactivity of these samples.

[1] To whom correspondence should be addressed. E-mail: jcconesa@icp.csic.es.

0021-9517/00 $35.00

METHODS

The ZSM-5 zeolite was prepared in the presence of propylamine template and calcined in air at 823 K to obtain the hydrogen form. The Si/Al ratio was 25.1 and the Al content was 0.64 mmol g^{-1}, with an ion-exchange capacity of 0.60 mmol NH_4^+ g^{-1}. Two samples containing about 2 wt% copper were prepared. One sample (SR) was ion exchanged via solid-state reaction between H-ZSM-5 and CuO: the fine powders of the zeolite and the copper compound were thoroughly mixed and heated, at 10 K min^{-1} ramp rate, in a stream of nitrogen up to 873 K, and were then kept at the same temperature for 1 h. For the liquid solution ion-exchanged sample (LS), H-ZSM-5 was first converted to the sodium form by titrating the zeolite with a 0.1 *M* NaOH solution, and then the sample was washed and dried. A 5.4 g amount of this Na-ZSM-5 was stirred in a 350 cm^3 solution of 0.01 *M* $Cu(CH_3COO)_2$ during 5 h and centrifuged, this procedure being repeated twice, finally, the material was washed with distilled water and dried in air at 353 K. The compositions of both catalysts, measured by atomic absorption, were very similar: [Cu] = 0.30 mmol g^{-1}, [Al] = 0.63 mmol g^{-1} (thus, Cu/Al ratio = 0.48). Sample LS contained only residual sodium ([Na] = 0.01 mmol g^{-1}).

EPR spectra were recorded at 77 and 298 K with a Bruker ER-200D spectrometer, operating in X-band and calibrated with a DPPH standard ($g = 2.0036$). Portions of the samples, about 20 mg, were placed in a quartz probe cell with double greaseless valves, using a conventional high-vacuum line for the outgassing and gas adsorption treatments. NO adsorption was carried out by introducing a known gas pressure in the volume between two cell valves (ca. 5 cm^3, corresponding to 0.26 μmol/Torr; 1 Torr = 133.3 N m^{-2}) and expanding it to the sample cell. In a typical low-dose experiment, 5 Torr of NO are expanded over the sample. The unpaired electrons detected in the spectra were quantitated by comparing the corresponding doubly integrated intensities with that of a copper sulfate standard. To determine the signal parameters with higher accuracy and separate the contributions of the signals when they appear overlapped, computer simulations were carried out, using an in-house program based on standard second-order perturbation formulas or, when nuclear quadrupole coupling had to be included, an adaptation of the program QPOW (10) based on exact diagonalization of the spin Hamiltonian.

RESULTS

The EPR spectra obtained for the Cu-ZSM5 samples subjected to varied treatments presented several signals ascribable to copper species. The corresponding EPR parameters, together with ligand field parameters derived from them (see Discussion), are presented in Table 1. In all cases the EPR parameters presented in this table are derived from computer simulations, rather than from direct measurements of peak positions; as is well known (11), the latter are influenced (mainly in the high field region) by the presence of extra singularities and by the effects of nuclear quadrupole coupling, which may lead to changes in peak amplitudes and to the appearance of "forbidden" transitions (involving change in the nuclear quantum number M_I) between the high-field peaks. Table 1 also includes values of ligand field parameters obtained from the EPR values as explained in the Discussion. Note that, although the spectra afford absolute values only for the A and Q parameters,

TABLE 1

Spin-Hamiltonian Parameters and Ligand Field Parameters Obtained from Them, Determined for the EPR Signals Found in the Cu-ZSM5 Samples

	EPR parameters (A and Q values in units of 10^{-3} cm^{-1} or [Gauss])						Ligand field parameters		
Signals	$g_\parallel$	$g_\perp$	$\langle g \rangle$	$A_\parallel$	$A_\perp$	$\lvert Q \rvert$	Δ_{xy}/λ	δ/λ	α^2
I			~2.19						
A′	2.386	2.082	2.1833	−15.15 [136]	~−0.9 [9]	nd	18.0	3.6	0.892
A″	2.398	~2.08	~2.186	−14.0 [125]	nd	nd	16.8	~3.4	nd
B	2.343	2.0665	2.159	−17.2 [157]	−1.5 [15.5]	0.45	20.3	6.3	0.893
C′	2.329	2.063	2.152	−15.5 [142]	−1.8 [18.5]	nd	19.2	6.7	0.822
C″	2.355	~2.063	~2.161	−15.5 [144]	~−1.8 [18.5]	nd	18.5	~8.3	~0.847
C‴	2.314	2.059	2.144	−16.85 [156]	−1.35 [14]	0.35	21.2	7.8	0.858
D′	2.281	2.0535	2.1295	−17.9 [168]	−2.05 [21.5]	nd	23.0	8.3	0.831
D″	2.280	2.055	2.13	−18.5 [174]	−2.1 [22]	<0.2	23.5	7.5	0.850
OI			~2.4						
OII	$g_1 = 2.265$		$g_2 = 2.125$	$g_3 = 2.075$		$\langle g \rangle = 2.155$			
N	$g_1 = 2.0035$ $A(Cu)_1 = 14.5$ [155]		$g_2 = 1.9975$ $A(Cu)_2 = 16.0$ [171] $A(N)_2 = 2.6$ [28]		$g_3 = 1.8845$ $A(Cu)_3 = 16.8$ [191]				

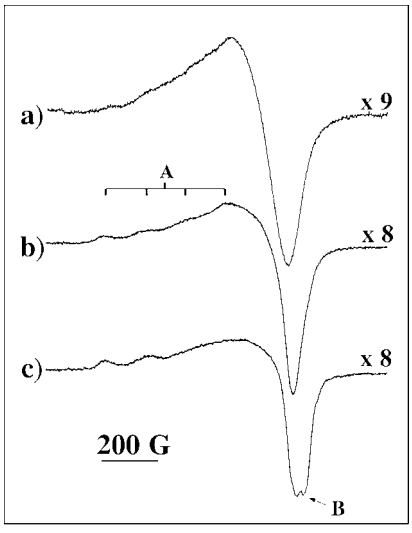

FIG. 1. EPR spectra at 298 K of sample LS: hydrated (a) and outgassed at 298 K at 10^{-3} Torr (b) and at 10^{-4} Torr (c).

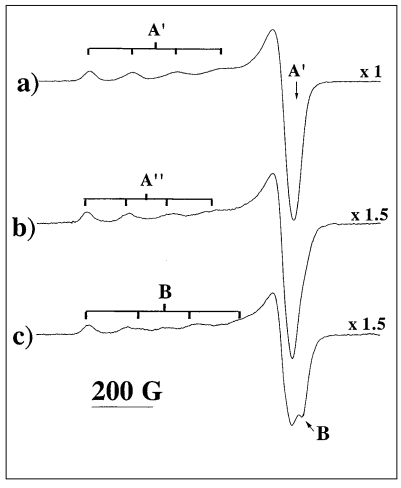

FIG. 2. EPR spectra at 77 K of sample LS: hydrated (a) and outgassed at 298 K at 10^{-3} Torr (b) and at 10^{-4} Torr (c).

both $A_\parallel$ and $A_\perp$ are given in Table 1 with negative signs, as only then can they be compatible with acceptable values of ligand field parameters.

I. Effect of Outgassing Treatments on the Hydrated Cu-ZSM-5

A. Sample Prepared by Liquid Solution Ion Exchange

The EPR spectrum of the hydrated sample LS, recorded at $T_m = 298$ K (Fig. 1a), showed mainly a broad non-isotropic signal without hyperfine structure, denoted here as type I, with extrema at $g = 2.24$ and 2.11. Individual principal values of the **g** tensor are not resolved; several computer simulations representing (imperfectly) the obtained shape yield average g values around 2.19. The observation of a hyperfine structure (hfs) of several equispaced weak peaks at the low-field side of the spectrum, with positions corresponding to parameters $g = 2.340$ and $A = 125$ G, indicates the presence of a second minor signal. The spectrum-integrated intensity corresponded to 95% of the total sample copper content. When the sample is cooled at 77 K, signal I is no longer observed, and the spectrum, Fig. 2a, is formed mainly by an axial signal A' with $g_\parallel = 2.386$, $g_\perp = 2.082$, $A_\parallel = 136$ G, and $A_\perp = 9$ G (the latter splitting was not resolved but could be estimated via computer simulation, as it determines the relationship between the tail slopes and peak-to-peak widths of the high-field feature).

After mild outgassing (10^{-3} Torr) for 1 h at $T_v = 298$ K, the spectrum obtained at $T_m = 298$ K, Fig. 1b, was formed by a type I signal, with shifted extrema and lower intensity than before outgassing, overlapping a partially resolved A type signal that appeared with $g_\parallel = 2.370$ and $A_\parallel = 125$ G; its $g_\perp$ and $A_\perp$ parameters are not resolved. The total integrated intensity of this spectrum corresponded to 69% of the total copper present. The spectrum obtained at $T_m = 77$ K (Fig. 2b) was formed by an overlapping of signal A' (with lower intensity than in the hydrated sample) and another similar one (A'') with $g_\parallel = 2.398$ and $A_\parallel = 125$ G; again, for this latter signal $g_\perp$ and $A_\perp$ could not be resolved, as the corresponding features overlapped those of signal A'.

A somewhat deeper outgassing (achieving a residual pressure of 10^{-4} Torr) at 298 K produced significant modifications in the spectra, as well as an additional decrease of the intensity, that now reaches a value equivalent to 59% of the total copper. For $T_m = 298$ K, the spectrum (Fig. 1c) showed a new peak at high field evidencing a new signal with a $g_\perp$ value lower than that of A type signals; for $T_m = 77$ K, Fig. 2c, this new signal (B) appeared better resolved. Further outgassing at temperatures of 323 and 353 K led to a decrease, until practical vanishing, of signals I and type A, with almost exclusively signal B remaining, Figs. 3a,b

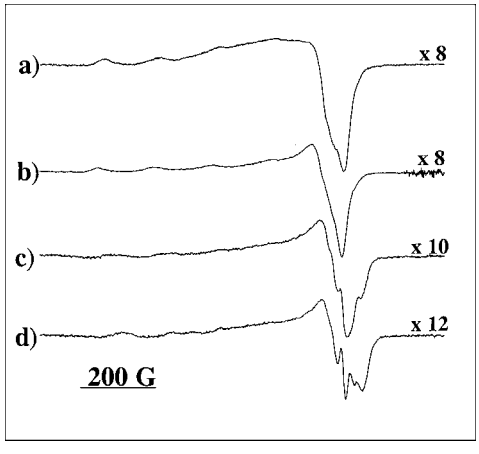

FIG. 3. EPR spectra at 298 K of sample LS outgassed at $T_v =$ 323 K (a), 353 K (b), 383 K (c), and 413 K (d).

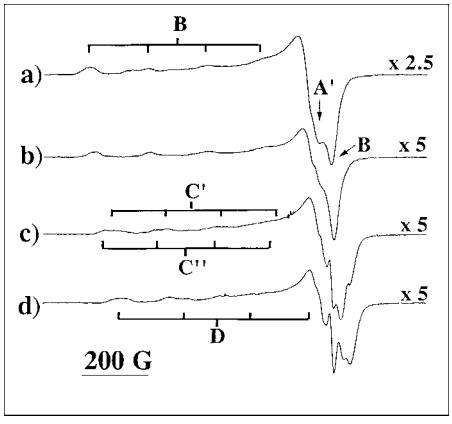

FIG. 4. EPR spectra at 77 K of sample LS outgassed at $T_v = 323$ K (a), 353 K (b), 383 K (c), and 413 K (d).

and 4a,b. This allowed us to determine the EPR parameters (given in Table 1) with higher accuracy, including a nonnegligible nuclear quadrupole coupling Q which had to be introduced to achieve good simulation of the high-field features. It is noted that the integrated intensities of the spectra shown in Figs. 3a and 4a and in 3b and 4b correspond to 56% and 27% of the total copper, respectively. The evolution of the spectrum intensity with increasing T_v is shown in Fig. 5.

Heating the sample *in vacuo* at 383 K did not produce any further significant decrease of the spectrum integrated intensity; the spectra obtained at $T_m = 298$ and 77 K (Figs. 3c and 4c) presented similar features, both of them being formed by signal B (now minority) and two new types of signals, denoted as C and D′, characterized by better resolved high-field components. For the C-type signal, the hyperfine-split quartet of the parallel component shows a broadening, and the high-field line of the latter appears to be split, indicating the presence of two slightly different signals type C in different amounts, named here C′ and C″, of which only the first remains at the highest outgassing temperature used; also, the improved resolution of the high-field part now allows determination at the hyperfine splitting constants $A_\perp$ for signal D′ and the main signal of type C (C′) (see Table 1), although their overlapping precludes verification of the presence of nuclear quadrupole coupling effects. Further outgassing at $T_v = 413$ K did not produce any significant change of the spectrum intensity; signal B practically disappeared, while the relative contribution of signal D′ to the spectrum increased, Figs. 3d and 4d.

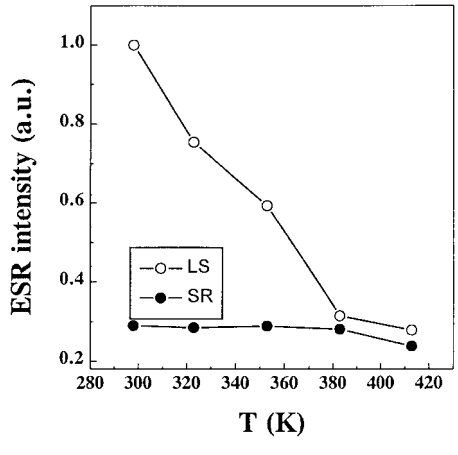

FIG. 5. Evolution of the spectrum intensity (recorded at $T_m = 298$ K) with increasing T_v for sample LS (a) and SR (b).

B. Sample Prepared by Solid State Reaction

A similar study of the effect of T_v on the EPR spectrum was carried out on sample SR. One important difference noted in this case is the presence of a very broad signal OI, Fig. 6, with $g \approx 2.4$ and width $\Delta H_{pp} \approx 2000$ G, which is observed clearly in all the spectra obtained at 298 K and is not significantly modified in shape by outgassing treatments. It is noted that decreasing the temperature to $T_m = 77$ K does not produce the expected ca. fourfold increase in the intensity of this signal due to the Boltzmann factor; rather, the signal is broadened so that its amplitude actually decreases. This indicates ferromagnetic-type behavior for the species producing this feature. No such line was ever observed in sample LS.

Together with this broad component, typical Cu^{2+} signals also appear, which are similar in shape and parameters to those detected for sample LS; their intensities, however, behave differently. In the initial hydrated state the integrated intensity of these signals accounts for only ca. 30% of the total copper present in the sample, and then remains nearly unchanged during outgassing at increasing temperatures, so that for $T_v = 383$ K it matches the value reached by sample LS; see Fig. 5. Apart from this, the transformations of these signals which occur upon outgassing of the sample at increasing T_v were relatively similar to those observed for sample LS (spectra not shown). Some small

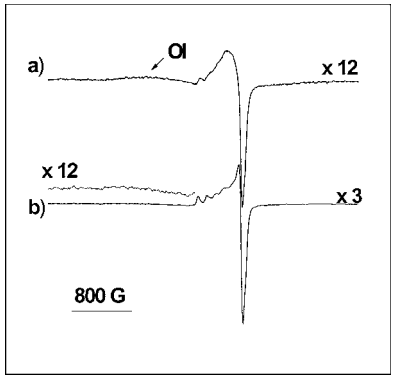

FIG. 6. EPR spectra of hydrated sample SR at 298 K (a) and 77 K (b).

variations in the values of the parameters of some signals, in relation to those of similar signals obtained for sample LS, were found necessary to improve the simulation of some of the spectra, but, in general, the results indicate that the same signals type A, B, C, and D′ are present and appear in similar sequences in the spectra of both samples. As main differences, it can be noted that the appearance of signal type B occurs at lower T_v for SR than for LS, while the total transformation of the species originating signals type A (mainly A′) to produce signal B required a higher T_v. Signal D′ also started to appear at higher T_v for SR than for LS, and always remained smaller than in this latter sample.

II. Effect of NO and/or O_2 Adsorption on the Samples Outgassed at 413 K

A. Sample Prepared by Liquid Solution Ion Exchange

O_2 adsorption (1 Torr) at 298 K on sample LS previously outgassed at 413 K (Fig. 7a) produced a decrease of the spectrum intensity, due to the decrease of C-type and D′ signals, that is not compensated for by the formation of any new signal (Fig. 7b). This may be due simply to broadening of the signals by dipolar magnetic interaction with the physisorbed oxygen molecule; indeed, reoutgassing at RT reversed the effects produced by the contact with O_2, showing that no significant redox reactivity is involved in this interaction.

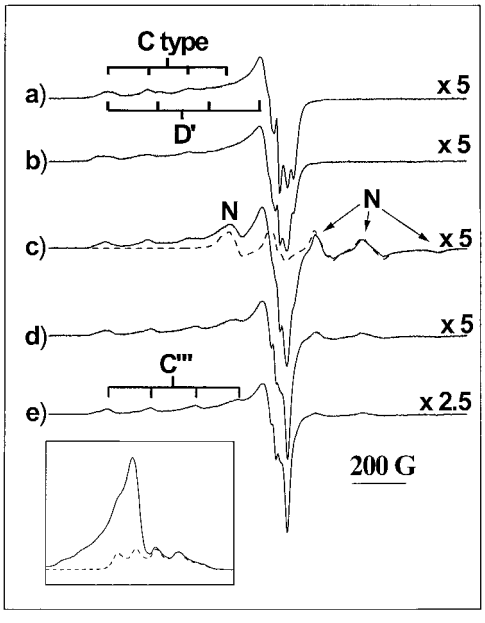

FIG. 7. EPR spectra at 77 K of sample LS outgassed at 413 K (a) and contacted with O_2 (1 Torr) (b). Contacted with NO (5 Torr) at 298 K after outgassing at 413 K (c), contacted at 298 K with 20 Torr of NO (d), and subsequently outgassed at 298 K (e).

NO adsorption (5 Torr) at 77 K on the sample outgassed at 413 K (displaying a spectrum with integrated intensity corresponding to 27% of total Cu) produced a small decrease of spectrum intensity that affected both C- and D′-type signals. When the sample was warmed in the closed cell at 298 K for 5 min (Fig. 7c), signal D′ strongly decreased. Signal C also decreased somewhat, but the total spectrum intensity did not decrease (rather, it increased a little, recovering the 26% level); this was due to the formation of a new signal N, with $g_x = 2.0035$, $g_y = 1.9975$, and $g_z = 1.8845$, and displaying two superimposed hyperfine splittings: one of four lines, with coupling constants $A_x = 14.5 \times 10^{-3}$ cm^{-1}, $A_y = 16.0 \times 10^{-3}$ cm^{-1}, $A_z = 16.8 \times 10^{-3}$ cm^{-1}, and another one of three lines (coupling to N, $I = 1$) with $A_x^N = 0.4 \times 10^{-3}$ cm^{-1}, $A_y^N = 2.6 \times 10^{-3}$, and $A_z^N = 0.45 \times 10^{-3}$ cm^{-1}. Computer simulations reproducing the shape of this spectrum (see dashed line in Fig. 7c) indicated that this latter signal represents about 30% of the total integrated intensity of the spectrum in Fig. 7c; this is visualized in the single integral of the spectrum (absorption curve), see inset in Fig. 7. It was noted that after the sample had been left within the closed cell at room temperature for several hours the spectrum increased significantly in intensity (up to 33% of Cu content), due mostly to an increase in signal type C.

NO was adsorbed also in higher and lower amounts. Thus, in one experiment a small NO pressure (below 1 Torr), corresponding to ca. 0.04 mmol · g^{-1}, was contacted with a portion of sample LS preoutgassed at 413 K, which displayed (before NO adsorption) a spectrum with an intensity accounting for 20% of the total Cu present. After contact with NO for 5 min at RT, signal N developed to almost the same extent as in the experiment with 5 Torr of NO described above, the total integrated intensity of the EPR signal then reflecting spins equivalent to 22% of the total Cu present in the sample. Keeping the sample at the same temperature for 2 h increased the spectrum intensity appreciably (again, mainly that of the signal type C component; signal N remained almost unchanged), up to the equivalent of 25% of the copper present.

Adsorption of a higher amount of NO (a 20-Torr dose), on the other hand, produced a greater decrease in spectrum intensity, mainly of signal type C, but also of signal N, the contribution of which now represented ca. 25% of the total integrated intensity (Fig. 7d). Outgassing at 298 K produced an increase of the spectrum intensity (due to an increase in signal type C, as signal N was unchanged); its value, now corresponding to 36% of the total copper content, was higher than that observed previous to the NO adsorption (27%). The spectrum is now formed mainly by a signal type C (named C′′′), a smaller signal C′ and signal N (Fig. 7e). Subtraction of the spectra in Fig. 7d and e isolates the shape of signal C′′′; computer simulation then allows us to measure its g and A parameters accurately, to verify the

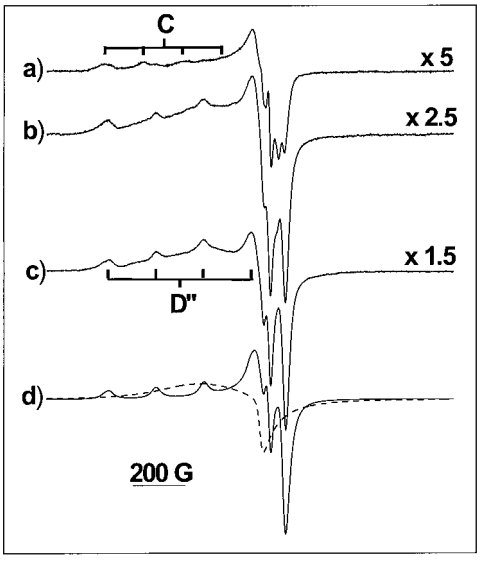

FIG. 8. EPR spectra at 77 K of sample LS outgassed at 413 K (a), contacted with NO (30 Torr) and O_2 (15 Torr) at 298 K for 5 min (b) and after subsequent outgassing at 298 K (c). (d) Computer-simulated signals D″ and OII which best reproduces spectrum c.

presence of nuclear quadrupole coupling effects in this signal and to estimate the value of the corresponding constant Q (Table 1).

Adsorption at 77 K of a mixture of NO (30 Torr) and O_2 (15 Torr) on sample LS outgassed at 413 K (Fig. 8a) produced a decrease of the spectrum intensity; however, after the sample was warmed at 298 K, the spectrum intensity showed a fast increase (up to 70%) during the first few minutes (Fig. 8b) and a slower one afterward. Outgassing at 298 K produced an additional increase, so that now 90% of the total copper was detected as Cu^{2+} (Fig. 8c). This detection of almost all the existing copper as Cu^{2+} species is observed not only in the form of an increase of the signals of isolated Cu^{2+} cations (mainly as a type D signal, which we name D″, together with a smaller contribution of type C signals), but also by the formation of a new broad signal OII (Fig. 8d). The shape of this signal can be estimated approximately by subtracting from the spectrum in Fig. 8d the shape (computer-simulated) of signal D″; the difference spectrum, which can best be reproduced with parameters $g_1 = 2.265$, $g_2 = 2.125$, and $g_3 = 2.075$, does not present any resolved hyperfine splitting. Figure 8e displays the shapes of the signals D″ (well resolved) and OII (broad), which give a good simulation of this experimental spectrum. It was noted that signal D″ was best reproduced without including significant nuclear quadrupole interaction in the simulation.

B. Sample Prepared by Solid-State Reaction Ion Exchange

Experiments involving NO adsorption were carried out also on sample SR, producing signals with shapes similar to those observed for sample LS (spectra not shown). NO adsorption (5 Torr dose) at 77 K on the sample preoutgassed at 413 K produced an important decrease of the spectrum intensity, due to the decrease of signals C and D′; an intensity recovery is observed on warming the sample at 298 K, with the simultaneous formation of signal N. Signal OI did not show any significant modification in this process. Outgassing at 298 K produced an increase in spectrum intensity, to reach a value a little higher than that obtained previous to the NO adsorption. The spectrum is formed mainly by signals C‴, C′, and N.

Adsorption at 77 K of a mixture of NO and O_2 on sample SR, outgassed at 413 K, produced a significant decrease of the spectrum intensity as in the case of sample LS, but, after warming at 298 K, there was no important intensity increase. After outgassing at 298 K, the spectrum was again dominated by the sharp features of a D-type signal, as in sample LS, but differed from the latter in that its integrated intensity was only a little higher than before adsorption of the $NO + O_2$ mixture.

DISCUSSION

I. Effects of Outgassing

The overall evolution of the ESR spectra observed here for sample LS upon outgassing at room or moderate temperatures, and the corresponding interpretation, are in accordance with those reported in previous literature works for ZSM-5 (or other zeolites) exchanged with Cu^{2+} (5–9, 12). Thus, the relatively broad spectrum recorded at RT for the hydrated specimen, in which neither hyperfine structure splitting nor features corresponding to individual g values are resolved, corresponds to fully hydrated, sixfold coordinated Cu^{2+} ions. In principle, these will have their octahedral ligand coordination distorted (tetragonally elongated) due to a Jahn–Teller effect, giving rise to an asymmetric EPR spectrum with axial-type shape, but a fast tumbling movement (or a reorientation of the distortion axis) of the complex in the near-liquid environment of the completely hydrated zeolite pores tends to average the **g** tensor components and obliterates the hyperfine splitting. Upon freezing at 77 K, this tumbling or reorientation stops and a typical anisotropic (axial) spectrum, with well-resolved hyperfine structure at least in the parallel component, is observed. Signal integration indicates that such a spectrum essentially accounts for all copper present; thus di- or polynuclear hydroxide-bridged species, which are known to occur in moderately alkaline solutions and which would not produce such an ESR spectrum, are not present here to a significant extent.

Probably, those mononuclear hydrated species are not located in the zeolite channels themselves; the internal dimensions of these, around 0.53 nm free diameter, are possibly too narrow to contain without restrictions the larger

$[Cu(H_2O)_6]^{2+}$ ions (with equivalent diameter presumably above 0.6 nm). These are more likely to lie at the intersections of these channels, which provide more room to accomodate such complexes, although probably not more than one of them at a time. Note that there are four such intersections per unit cell, so that the composition of the sample, containing 3.7 Al ions/unit cell, implies the presence of 0.45 Cu ions per channel intersection. The noticeable asymmetric character of the RT spectrum indicates that the mentioned averaging is not complete; this may be due simply to some hindrance to rotation suffered by the hydrated ions in the cavities or when they approach the channel openings. Indeed the shape of the observed spectrum is not so close to the shape of an isotropic spectrum as that observed in wider pore zeolites such as Y (12). One additional reason for such an effect, in zeolites with higher Si/Al ratio and therefore with a more sparse spatial distribution of Al sites, could be imperfect compensation of the internal electric fields when two monovalent cations are substituted by a divalent one, which may lead to stronger electrostatic interactions on the copper complex, further affecting its movement.

Gradual desorption of water upon outgassing at room or higher temperatures leads first to disappearance of the liquid-like environment, so that the complex no longer tumbles but is immobilized on the zeolite pore walls; further elimination of water leads to direct bonding of the Cu ion to zeolite framework oxygens (these replacing some of the lost water ligands) and eventually to a decrease in the coordination of copper, giving typically square pyramidal or square planar geometries. For these, the EPR spectra would have in all cases shapes characteristic of axial (tetragonal) symmetry, which corresponds to the unpaired electron located mostly in a $d(x^2-y^2)$ orbital of the Cu ion. It must be noted that, although initially only $[Cu(H_2O)_n]^{2+}$ species are expected to occur with at most small amounts of hydrolized $[Cu(H_2O)_{n-1}(OH)]^{+}$ ions [which require moderately alkaline solutions or overexchange conditions during preparation (7, 13)], such hydrolysis might occur during thermal dehydration, allowing detached protons to spread over the lattice and thus neutralize more effectively the overall framework negative charge, less shielded after elimination of the aqueous dielectric medium. Thus some of the detected species could be of $[Cu(H_2O)_x(OH)]^{+}$ type.

The changes in coordination are reflected in the values of the EPR parameters observed, which can be used to characterize the ligand field environment of the species involved. Accurate relationships between these parameters and the molecular orbital compositions and energies can be established through complex expressions which may involve a number of variables (14). Here we will use the more practical expressions given by Kivelson and Neiman for d^9 ions in D_{4h} symmetry (15) and will further simplify them by assuming that the only significant covalency effects reside in the mixing between the $d(x^2-y^2)$ orbital of the Cu ion and the corresponding symmetry-adapted combination of ligand orbitals. One then obtains

$$A_\parallel = -P[\alpha^2(\kappa_0 + 4/7) - (\Delta g_\parallel + 3\Delta g_\perp/7)(1+\tau)],$$
$$A_\perp = -P[\alpha^2(\kappa_0 - 2/7) - (11\Delta g_\perp/14)(1+\tau)],$$

with

$$\tau = \alpha' S/(\alpha - \alpha' S),$$
$$\Delta g_\parallel = g_\parallel - 2,$$
$$\Delta g_\perp = g_\perp - 2.$$

Here $P = 2\beta_e\beta_N\langle r^{-3}\rangle$ (for the half-occupied orbital), κ_0 is the Fermi contact term of the Cu^{2+} ion (with a value normally around 3/7), α and α' are the respective coefficients of the copper $d(x^2-y^2)$ and ligand-combination contributions to the semioccupied orbital, and S is the overlap between the latter; α, α', and S are linked by the normalization condition

$$\alpha^2 + \alpha'^2 - 2\alpha\alpha' S = 1.$$

Thus the parameter α^2, describing the $d(x^2-y^2)$ character of the unpaired electron and thus the covalency of the Cu–ligand bond ($\alpha^2 = 1$ means no covalent character at all), can be computed from the g and A values. Also, within the same approximation scheme,

$$g_\parallel - g_e = -8[\alpha^2/(1+\tau)]/(\Delta_{xy}/\lambda),$$
$$g_\perp - g_e = -2[\alpha^2/(1+\tau)]/(\Delta_{xz}/\lambda),$$

where λ is the Cu^{2+} spin–orbit coupling constant for the d orbitals, and Δ_{xy} and Δ_{xz} are the energy separation between the semioccupied $d(x^2-y^2)$ and the filled d_{xy} and (d_{xz}, d_{yz}) orbitals, respectively. Δ_{xy} is a measure of the ligand field (in the equatorial plane), while the tetragonal distortion can be quantified with $\delta = (\Delta_{xy} - \Delta_{xz})$, equal to the difference in energy between the d_{xy} and (d_{xz}, d_{yz}) orbitals.

Thus, using the values (15) $P = 0.036\ cm^{-1}$, $S = 0.076$ (for oxygen-type ligands; results are not very sensitive to this parameter here), and $\lambda = -828\ cm^{-1}$ (the free ion value), one can obtain α^2, Δ_{xy}, and δ; the corresponding values (with Δ_{xy} and δ given in units of $|\lambda|$) are included in Table 1.

The general trend observed upon outgassing indicates an increase in ligand bond covalency (decrease in α^2), in ligand field (Δ_{xy}), and in distortion from octahedral symmetry (δ). Several groups can be discerned on the basis of the ligand parameters. Type-A signals, ascribable to hexacoordinated species, have low δ and high α^2; type-D signals correspond to square planar geometries, and have high Δ_{xy} and low Q (the lack of axial ligands pushes the equatorial ones toward the cation, increasing the ligand field and balancing better the intraatomic quadrupole field of the $d(x^2-y^2)$ hole).

Type-C signals with intermediate Δ_{xy} can be ascribed to square pyramidal geometry. Signal B is less easy to ascribe, as its crystal field parameters Δ_{xy} and δ are similar to those of the species with square pyramidal geometry, but the lower covalency degree and higher quadrupole coupling make it closer to that of the hexacoordinated species giving type-A signals. Since B-type species (the only ones detected at the $T_v = 353$ K stage) produce upon dehydration the square pyramidal species C (and subsequently species D), one possibility is to ascribe them to hexacoordinated species, which would differ from A-type species in having a higher number of zeolite oxygen atoms in their coordination environment. The alternative is to ascribe them to pentacoordinated species where the number of water molecules and the number of zeolite oxygens in the coordination sphere are respectively larger and smaller than those of C-type species. Both would agree with the EPR-ESEM data by Anderson and Kevan which show that, after prolonged evacuation at RT of a Cu-exchanged Na-ZSM5 zeolite (a situation which produces here mainly signal B), the main species detected is coordinated to three water ligands.

Apart from these considerations on the observed ESR spectra, an important point concerns the signal intensities measured. For sample LS these indicate that, as soon as water elimination by outgassing begins, some Cu^{2+} ions (all of them initially observable by EPR) are transformed into species which escape EPR detection; the minimum integrated signal intensity is reached for outgassing temperatures of ca. 385 K. A decrease in the EPR signal intensity of Cu^{2+} in ZSM-5 zeolite upon outgassing has been reported in previous works (7, 13). The same effect was reported by us some time ago for Cu-exchanged Y zeolite (16); a relevant fact, observed in this latter work as well as in the results reported by LoJacono *et al.* (13) for Cu-ZSM-5, is that measurements of the magnetic susceptibility indicated in both cases no loss in this observable during this process. In fact, the T-dependent magnetic data obtained in (13) followed a pure Curie law, indicating that all Cu ions behaved essentially as paramagnetic species without experiencing significant ferro- or antiferromagnetic interactions; comparison of inverse magnetic susceptibility plots presented by those authors clearly indicates that the decrease in susceptibility found in that work for outgassing temperatures at least up to 423 K is not larger than ca. 5%. Thus the important decrease in EPR signal (down to less than 20% of the initial value in some cases) is not due to reduction of Cu^{2+} to Cu^{+} (or lower) redox state, nor to coupling of the unpaired electrons into a paired or other strongly magnetically interacting state. In our earlier work it was ascribed to positioning of Cu^{2+} in some of the 3-fold cation positions of the Y zeolite, which together with a specific water ligand location led to trigonal symmetry with a nearly degenerate ground state and strong spin–lattice relaxation (due to the presence of low-lying excited states) so that the EPR signal was broadened beyond detection.

In the present case, such an interpretation is less easy to justify, as ZSM-5 has intrinsically no trigonal symmetry sites. Possibly in some cases, i.e., for some combination(s) of water/zeolite ligands numbers and positions, these latter adjust themselves so that a near-degenerate ground state with spin–lattice relaxation characteristics similar to those mentioned above appears. However, it is noted that undetectable copper is not only formed in the sample only briefly outgassed at RT in which mobility of the visible Cu^{2+} (Fig. 1b), all of it hexacoordinated, indicates that a significant amount of near-liquid water still exists; it is also formed (and represents most of the copper) in the sample outgassed at 413 K, in which square-planar and square-pyramidal Cu^{2+} ions coexist. It does not seem probable that the EPR-invisible Cu^{2+} may have the same coordination in both situations, so the explanation of this undetectability in terms of a fast spin–lattice relaxation due to specific coordination symmetry seems again little likely. An alternative explanation would assume that, with a decrease in the number of water molecules, some interaction between Cu^{2+} ions appears, e.g., via Cu–(OH_2)---(OH)–Cu fluctuating hydrogen bonds, which leads to spin–spin relaxation via magnetic coupling (weak, as the Cu–Cu distance will be relatively large, easily of 0.5 nm or above), resulting again in a large broadening of the spectra. This interaction might be conserved even if the number of coordinated water molecules changed (so long as some of them remain to keep the hydrogen bond, if this latter is essential), thus explaining the possibility of having this effect for rather different degrees of sample hydration. In any case, further work still needs to be done to achieve a definitive interpretation of this fact.

Overall, the results indicate that, upon prolonged low-temperature outgassing, in a first stage (below ca. 350 K) hexa- (and maybe penta-)coordinated Cu species strongly bound to the zeolite lattice and detectable by EPR appear while simultaneously other Cu ions transform into paramagnetic but EPR-undetectable species, and later on some part of those hexacoordinated cations transform into the undetectable form while the rest end up as detectable square pyramidal and planar species. This makes it likely that the undetectable species are also five- or four-coordinated complexes, but further details cannot be given from these data.

II. Effects of NO Adsorption

Adsorption of NO at room temperature leads to the generation of the new species N while Cu^{2+} species decrease, especially signal D, which practically disappears. A signal quite similar to N was found by Giamello and Sojka *et al.* (17) upon reaction of NO with a ZSM-5 zeolite containing Cu^{+}, being ascribed there to a $(Cu–NO)^{+}$ complex with

the unpaired electron residing mostly on the N atom. This species was found by these authors to be detectable also by IR spectroscopy through a characteristic band located at 1811 cm^{-1}.

In our case, one first point to discuss is whether signal N could arise from Cu^+ ions existing prior to NO adsorption. Our results do not allow us to verify directly whether such Cu^+ was present just before NO adsorption, and cannot therefore give a conclusive answer in this respect. However, we may recall that, as mentioned above, the results of Lo Jacono *et al.* (13) indicate that the amount of Cu^{+2} which may be reduced to Cu^+ by outgassing at the low temperature used here (413 K) should be less than ca. 5%; the total amount of spins represented by signal N which are found here (Fig. 7) corresponds to ca. 8% of the total Cu present in the sample. This figure seems noticeably higher than that deduced from the work of Lo Jacono *et al.* On the other hand, the change found here in the overall integrated intensity of the spectrum upon NO adsorption at room temperature is substantially smaller than the amount of the new signal N formed. This means that the amount of signal N found is rather similar to the amount of Cu^{2+} which has disappeared from the spectrum, which hints at a cause-to-effect relationship rather than to a casual fact.

These two observations together suggest that in our case the process could be described essentially as the formation of species N at the expense of Cu^{2+} species, mostly of the kind which previously produced signal D. This must then involve both reduction of Cu^{2+} by one NO molecule and interaction with a second NO, the first step being probably the formation of a weak Cu–NO adsorption complex (diamagnetic but detectable by IR) as is well known to occur in these systems (17),

$$Cu^{2+} + NO \Longleftrightarrow (Cu^{+}\text{–}NO^{+}), \qquad [1]$$

followed by its reduction to form the EPR-visible complex,

$$(Cu^{+}\text{---}NO^{+}) + NO \rightarrow (Cu\text{–}NO)^{+} + NO^{+}. \qquad [2]$$

The fate of the NO^+ species thus formed is unclear. It probably does not stay as a second NO^+ ligand coordinated to the Cu ion; if it did, the Cu^+–NO complex formed would probably have ESR parameters different from those reported in (17) and would show hyperfine coupling to two N nuclei. More likely it gives rise to HNO_2 or nitrites upon interaction with remaining water or OH^- groups via a process such as

$$NO^{+} + H_2O \rightarrow HNO_2 + H^{+}. \qquad [3]$$

It must be noted that reaction [3] might occur concerted with [2], i.e., that the elimination of NO^+ could occur through interaction with water (or OH^-), so isolated NO^+ would not need to appear. Also, the elimination of NO^+ (water-assisted or not) might occur before the reaction with the second NO molecule, i.e., with intermediate production of Cu^+ which would subsequently produce the paramagnetic $(Cu\text{–}NO)^+$ complex. It is particularly interesting to note that these reactions seem to affect the square pyramidal species which give EPR signal C much less than the four-coordinated ones.

To our knowledge, such EPR detection of a $(Cu\text{–}NO)^+$ complex upon NO adsorption on Cu^{2+} species has not been reported previously. However, the work in Ref. (17a) does show that, when an oxidized Cu-ZSM5 sample (i.e., one which was outgassed at 873 K, in contact with O_2 at 673 K for 1 h, cooled to 298 K, and finally outgassed at 298 K), which can be assumed to contain no Cu^+, was contacted at 298 K with NO (0.07 Torr and above), the IR spectrum showed, together with the band at 1912 cm^{-1} characteristic of the $(Cu\text{–}NO)^{2+}$ species, a small amount of the band at 1811 cm^{-1}, indicating formation of $(Cu\text{–}NO)^+$ and thus showing that the latter species can form (even if in small amounts) upon NO adsorption on samples which should contain no Cu^+. This would agree with the mechanism given above; in this case, in which the material has been thoroughly dehydrated, O^{2-} ions (possibly incorporated into small CuO_x clusters) resulting from the oxidizing treatment could play the role of water (or OH^-) for reaction [3] above, NO_2^- ions being produced in this case. Unfortunately, that work did not mention whether the EPR spectra in this situation (which were not shown) displayed the signal due to the latter complex with significant intensity.

In any case, if other works in the literature, involving NO adsorption on samples containing only Cu^{2+}, failed to reveal the $(Cu\text{–}NO)^+$ species, this would not necessarily disprove the mechanism proposed above, since NO adsorption experiments are most frequently carried out on materials which have been thoroughly dehydrated by outgassing at temperatures higher than used here, and it might be that, as said above, water (or OH^-, or O^{2-} ions of some type produced only by oxidation) were necessary to remove the NO^+ species formed and complete the reaction effectively.

In principle, one cannot ensure from our spectra whether there is a chemical reaction between added NO and the EPR-undetectable Cu^{2+} species. Certainly no paramagnetic product seems to result. In addition, the fact that the above-described process leading to formation of complex $[Cu\text{–}NO]^+$ proceeds to a similar extent even if the amount of NO added is clearly smaller than the amount of undetected copper shows that, if some reaction of the latter with NO ever takes place at RT, it only happens after the reaction of NO with the EPR-detectable copper has been completed. The impression is, rather, that the EPR-undetected copper does not react with NO at RT. In view of the unreactive character of type C species toward NO, it seems reasonable to hypothesize that the undetectable ones are not four-coordinated but five-coordinated. The possibility

that they correspond to some type of trigonal bipyramid (to explain their undetectability via the trigonal symmetry alternative) remains open.

Reaction of the undetected copper does seem to occur at RT in a slower process taking place after the formation of the $(Cu–NO)^+$. In a reaction lasting 1 h or more, the total intensity of the spectrum increases, implying that some previously undetected copper has changed to a situation where EPR detects it, mostly as a C-type signal (i.e., a square pyramidal species). The amount of additional Cu appearing in the spectrum is never a large fraction, even if the amount of NO added is largely in excess; rather, it is similar to the amount of $(Cu–NO)^+$ complex initially formed. It seems thus likely that this increase results from a reaction between some of the additional products being formed in processes [1]–[3] above and the undetected Cu species, producing in the latter a change in coordination or a breaking in the interaction between Cu ions (in case the latter were the origin of the undetectability of Cu^{2+}). Here one should note that the type C species remaining after NO adsorption appear with lower intensity under NO pressure than after this latter is outgassed. This corresponds certainly to formation of a weak adsorption state of NO, according to step [1] above, which can be reversed by RT outgassing. The results here indicate that this weak bond quality applies to the five-coordinated species, not to the square complexes producing signal D′. Of course, it is possible that the EPR-undetectable species, which have been proposed above to have a five-coordinated structure, also act as sites for this weak type of adsorption, but this cannot be observed in our EPR experiments.

A remarkable fact is the complete transformation produced in the EPR spectrum upon contact of the previously outgassed sample with NO and O_2 at room temperature. First, the $(Cu–NO)^+$ complex disappears, and no N-containing radical products (such as NO_2) are seen. One possible process for this is the formation of peroxynitrite, an unstable species that, although able to generate some amounts of reactive radicals such as OH, mostly transfoms by isomerizing to the stable nitrate ion (18):

$$(Cu–NO)^+ + O_2 \rightarrow Cu^{2+} + ONOO^-, \qquad [4]$$

$$ONOO^- \rightarrow NO_3^-. \qquad [5]$$

Such reaction of a Cu^+–NO complex with O_2 to give a $Cu^{2+}–NO_3^-$ species is known in coordination chemistry (19), but of course there might be also other processes. Formation of nitrate during NO decomposition in these catalysts has indeed been indicated previously (20). Note that the several reaction steps [1]–[5] given above sum up to

$$2NO + H_2O + O_2 \rightarrow HNO_2 + NO_3^- + H^+, \qquad [6]$$

i.e., a Cu^{2+}-catalyzed oxidation of NO. Most notably, the C-type species, which scarcely react with NO alone, completely disappear; and furthermore, the integrated intensity of the final EPR spectrum now accounts for all the copper present. The resulting spectrum contains both a D-type signal, corresponding to a square planar species, and a less resolved signal; although a hyperfine structure cannot be discerned in this latter, and thus cannot be subjected to the theoretical analysis given above, it is noted that its average g value ($\langle g \rangle = 2.0155$) is closer to those of type-C signals, so a five-coordinated species seems more likely. The fact that these two signals appear with integrated intensities in ca. 1 : 1 proportion does not allow a simple formation scheme such as assuming that one of them results from the EPR-undetected species (which represented before the reaction more than 70% of the total copper) and the other one from (some of) the EPR-detected species.

Overall, it seems that all the Cu is transformed into one of these two species after the reaction with $NO + O_2$. One gets the impression that, once a ligand such as nitrate (or maybe nitrite) is formed, in a process catalyzed by low-coordinated Cu^{2+}, it interacts with all the copper present, producing new types of more stable Cu^{2+} complexes, all of which are EPR-detectable. Some of these exist as square planar isolated species giving well-resolved EPR signals, while others undergo mutual interactions leading to broadened signals in the spectrum. The broad lineshape of this latter signal suggests its ascription to Cu^{2+} species interacting via dipolar or weak exhange coupling, maybe mediated by a common bridging ligand. This, together with the possibility that the undetectability of part of the Cu^{2+} present is due to some weak Cu–Cu interaction, supports the idea that the structural and coordination circumstances in the zeolite may facilitate copper ions approaching and coupling to one another in different ways, depending on the type of ligands present, even if their concentration in the material is as low as here (less than 2 Cu ions per unit cell of volume = 5.36 nm^3). Indeed the possible relevance of coupled Cu pairs in these zeolites for the catalytic conversion of NO has been widely discussed (21).

III. Processes in the Specimen Prepared via Solid-State Reaction

The EPR spectra for sample SR show resolved signals which are quite similar to those in sample LS and appear or mutually transform at similar outgassing temperatures. Thus they can be ascribed to the same Cu^{2+} species. However, a notable difference is that, instead of having an intensity which initially corresponds to ca. 100% of the total Cu content and then decreases with dehydration to ca. 25% (as observed in sample LS), they represent this latter smaller fraction already in the starting air-equilibrated (and thus hydrated) state. The rest of the Cu^{2+} existing in this sample are probably in the state which gives the very broad

signal OI, although a quantitative correspondence cannot be established. The latter signal is likely to correspond to oligomeric Cu^{2+} species linked by oxidic bridges, which mediate ferromagnetic interactions between the cations; probably, the solid-state preparation method involves migration of $(CuO)_n$ species across the zeolite channels, which will become immobilized as clustered or isolated cations after combining with protons in reactions such as

$$(CuO)_n + 2H^+ \rightarrow (Cu_nO_{n-1})^{2+} + H_2O, \quad [7]$$

$$(CuO)_n + 2nH^+ \rightarrow nCu^{2+} + nH_2O, \quad [8]$$

and other similar processes, possibly including OH^- as well as oxide ions. One may thus hypothesize that the solid state preparation method leads to the location of isolated Cu^{2+} ions, via process [8], in some specific zeolite sites which are able to stabilize after dehydration EPR-detectable Cu^{2+} species, but which possibly exist in limited amounts, equivalent to only a fraction of the total Cu ions introduced. Then, the remaining Cu ions introduced in the solid state reaction as clusters would not be completely split as isolated ions, maybe because the other zeolite sites do not favor this breaking, and would remain as oligomeric species. Thus, after dehydration a similar (majority) fraction of Cu ions remain, in the LS sample, as EPR-undetectable ions, and in the SR sample as clusters producing a broadened signal.

The subsequent interaction with NO and O_2 reveals that, while the smaller fraction which gives well-resolved EPR spectra has similar chemical properties in both samples, the other larger fraction behaves differently, as it is not quickly transformed into species giving well-resolved signals in EPR. Thus one can conclude that this last transformation occurs quickly at room temperature only on nonclustered Cu ions; the clustered ones appear clearly less reactive than isolated Cu species. Even the EPR-silent species detected in sample LS, which do not react with NO alone at RT, are more reactive than these clusters, in view of their different behavior when contacted with the $NO + O_2$ mixture. This reduced reactivity of oxidic clustered species, lower than that of the not clustered ones present in sample LS (isolated or at most with weaker mutual interactions), might be the reason for the lower catalytic activity of sample SR in the NO decomposition reaction (4).

CONCLUSIONS

For sample LS, the outgassing treatments at increasing temperatures produce two effects on the EPR spectra: (i) modification of the coordination of isolated Cu^{2+} cations, first by substitution of lattice oxygen for water molecules in the initially octahedral coordination of the hydrated $[Cu^{2+}(H_2O)_6]$ complexes and subsequently by the further loss of ligand water molecules to reach square pyramidal or square planar coordination; (ii) formation, in this process of coordination change, of paramagnetic but EPR-silent Cu^{2+} species. This latter phenomenon, which for $T_v \geq 383$ K affects up to ca. 75% of the total copper and has been observed previously in zeolites Y (16) and ZSM-5 (13), may be due to a near-degenerate ground state or to weak spin coupling.

For sample SR, most of the copper forms small copper oxide clusters (observed as a very broad EPR line) that are not affected by the outgassing treatments and that take the place of the Cu^{2+} ions giving the EPR-silent species in sample LS. The amount and location of the rest of the Cu^{2+} cations (isolated) in this sample SR, and the modification of their coordination symmetry with increasing T_v, are not very different from those observed for the isolated Cu^{2+} cations in sample LS.

In sample LS, NO adsorbs at 298 K on Cu^{2+} cations with unsaturated coordination and reacts irreversibly with square planar Cu^{2+}; Cu^+–NO species appear as a result of this process, and it is proposed that they are formed from the four-coordinated Cu^{2+} in a two-step reaction with NO with possible assistance from remaining water or OH^- groups. Adsorption of a $NO–O_2$ mixture at 298 K produces the modification of nearly all of the Cu^{2+} species (EPR-silent or not), the resulting Cu^{2+} cations being detected either as square planar isolated Cu^{2+} species or as exchange-interacting Cu^{2+} ions.

In the case of sample SR, NO adsorption at 298 K produced similar effects on isolated Cu^{2+} cations as in the case of sample LS. Adsorption of a $NO–O_2$ mixture at 298 K did not alter significantly the copper oxide clusters, indicating that the reactivity of these associated Cu^{2+} cations is significantly lower and suggesting that such association in clusters may be connected with the lower catalytic activity of this sample in NO decomposition.

ACKNOWLEDGMENTS

Thanks are given to financial support from the CICYT (Project Nr. MAT97-0696-C02-01), the Comunidad de Madrid (Project Nr. 06M/085/96), and the CSIC-HAS bilateral agreement. A.M.-A. thanks the Comunidad de Madrid for a post-doctoral grant.

REFERENCES

1. Breck, D. W., "Zeolite Molecular Sieves: Structure, Chemistry and Use." Wiley, New York,1974.
2. Barrer, R. M., "Zeolites and Clay Minerals as Sorbents and Molecular Sieves." Academic Press, New York, 1978.
3. (a) Kucherov, A. V., and Slinkin, A. A., *J. Mol. Catal.* **90**, 323 (1994). (b) Kucherov, A. V., and Slinkin, A. A., *Zeolites* **6**, 175 (1986).
4. Schay, Z., Knözinger, H., Guczi, L., and Pál-Borbely, G., *Appl. Catal. B Environ.* **18**, 263 (1998).
5. Sendaka, Y., and Ono, Y., *Zeolites* **6**, 209 (1986).
6. Anderson, M. W., and Kevan, L., *J. Phys. Chem.* **91**, 4174 (1994).
7. Larsen, S. C., Aylov, A., Bell, A. T., and Reimer, J. A., *J. Phys. Chem.* **98**, 11,533 (1994).
8. Kucherov, A. V., Slinkin, A. A., Kodratev, D. A., Bondarenko, T. N., Rubinstein, A. M., and Minachev, Kh. M., *Zeolites* **5**, 320 (1985).
9. Kucherov, A. V., Gerlock, J. L., Jen, H. W., and Shelef, M., *J. Catal.* **152**, 63 (1995).

10. Program QPOW, furnished by The Illinois ESR Research Center, NIH Div. of Research Resources Grant No. RR01811; described in the following works: (a) Nilges, M. J., Ph.D. thesis, Univ. of Illinois, Urbana, Illinois, 1979; (b) Belford, R. L., and Nilges, M. J., Computer simulation of powder spectra, *presented at* EPR Symposium, 21st Rocky Mountain Conference, Denver, Colorado (1979); (c) Maurice, A. M., Ph.D. thesis, Univ. of Illinois, Urbana, Illinois, 1980.
11. (a) Conesa, J. C., and Soria, J., *J. Magn. Reson.* **33**, 295 (1979). (b) Rollmann, L. D., and Chan, S. I., *J. Chem. Phys.* **50**, 3416 (1969).
12. See e.g: (a) Conesa, J. C., and Soria, J., *J. Chem. Soc. Faraday Trans. I* **75**, 406 (1979). (b) Nicula, A., Stamires, D., and Turkevich, J., *J. Chem. Phys.* **1965**, 3684.
13. Lo Jacono, M., Fierro, G., Dragone, R., Feng, X., d'ltri, J., and Hall, W. K., *J. Phys. Chem. B* **101**, 1979 (1997).
14. Smith, D. W., *J. Chem. Soc. A* **1970**, 3108.
15. Kivelson, D., and Neiman, R., *J. Chem. Phys.* **35**, 149 (1961).
16. Conesa, J. C., and Soria, J., *J. Phys. Chem.* **82**, 1847 (1978).
17. (a) Giamello, E., Murphy, D., Magnacca, G., Morterra, C., Shioya, Y., Nomura, T., and Anpo, M., *J. Catal.* **136**, 510 (1992). (b) Sojka, Z., Che, M., and Giamello, E., *J. Phys. Chem. B* **101**, 4831 (1997).
18. (a) Stern, M. K., Jensen, M. P., and Kramer, K., *J. Am. Chem. Soc.* **118**, 8735 (1996). (b) Manuszak, M., and Koppenol, W. H., *Thermochim. Acta* **273**, 11 (1996).
19. Carrier, S. M., Ruggiero, C. E., Tolman, W. B., and Jameson, G. B., *J. Am. Chem. Soc.* **114**, 4407 (1992).
20. Schay, Z., Kiricsi, I., and Guczi, L., *Surf. Stud. Sci. Cat.* **116**, 347 (1998).
21. Lei, G. D., Adelman, B. J., Sarkany, J., and Sachtler, W. M. H., *Appl. Catal. B* **5**, 245 (1995).